Current Optics and Photonics
Vol. 1, No. 3, June 2017, pp. 233-238

ISSN: 2508-7266(Print) / ISSN: 2508-7274(Online)
DOI: https://doi.org/10.3807/COPP.2017.1.3.233

Gaussian Decomposition Method in Designing a Freeform Lens for an LED Fishing/Working Lamp

Anh Q. D. Nguyen[1], Vinh H. Nguyen[1], and Hsiao-Yi Lee[2]*

[1]Nguyen Tat Thanh University, Ho Chi Minh 702000, Vietnam
[2]Department of Electrical Engineering, National Kaohsiung University of Applied Sciences, Kaohsiung 80778, Taiwan

(Received December 1, 2016 : revised December 26, 2016 : accepted January 16, 2017)

In this paper we propose a freeform secondary lens for an LED fishing/working lamp (LFWL). This innovative LED lamp is used to replace the traditional HID fishing lamp, to satisfy the lighting demands of fishing and the on-board activities on fishing boats. To realize the freeform lens's geometry, Gaussian decomposition is involved in our optics-design process for approaching the targeted light intensity distribution curve (LIDC) of the LFWL lens. The simulated results show that the illumination on the deck, on the sea's surface, and underwater shows only small differences between LED fishing/working lamps and HID fishing lamps. Meanwhile, a lighting efficiency of 91% with just one third of the power consumption can be achieved, when the proposed LED fishing/working lamps are used instead of HID fishing lamps.

Keywords : Freeform lens, Light-emitting diodes, Gaussian decomposition, HID fishing lamp, Minimum mean square error
OCIS codes : (230.3670) Light-emitting diodes; (220.3630) Lenses; (150.2950) Illumination; (010.4450) Oceanic optics

I. INTRODUCTION

Recently, Light-emitting diodes (LEDs) have emerged as a contemporary technology to replace traditional lighting technologies in both civil life and industrial applications, due to their advantages such as high efficiency, long life-time, and fast response, as well as a reduced contribution to climate change [1-4]. However, contrary to that of conventional light sources like incandescent bulbs, the raw radiation pattern of LEDs is usually not favorable for specific lighting applications. Hence LEDs usually cannot be utilized by themselves.

The most popular solution to this problem is introducing an additional optical device, a secondary freeform lens, to convert the raw radiation pattern into a more suitable one [5]. The freeform surfaces of such lenses can produce uniform illumination and a proper intensity distribution. Chen et al. [6] have proposed a method for simple source-target luminous intensity mapping, to design a freeform lens for uniform LED illumination. Lin [7] has concentrated on how to solve the light-source misalignment problem that can cause large lamination variations through a such a lens. To achieve accuracy in an arbitrarily structured light pattern, Ma et al. [8] introduced an approach for designing a deconvolution freeform lens array that generates high-contrast, structured illumination patterns. Another freeform-lens design method has been proposed by Xie et al. [9], to enhance the brightness of a direct-lit LED backlight system.

The light-pattern design of LED light sources for undersea applications has been considered in recent years. In 2012, Shen and Huang [10] employed LED lights for attracting fish to replace traditional ones. The method for mapping light-intensity distribution curves onto horizontal and vertical planes was employed to design submodule lenses that produced a fish-attracting light pattern, with an alternating distribution of brightness and darkness. In 2014, Shen et

*Corresponding author: leehy@mail.ee.kuas.edu.tw
Color versions of one or more of the figures in this paper are available online.

al. [11] used Fourier series and an energy-mapping method to design a novel lens that produces a light pattern of multiple concentric circles to attract shoals of fish.

The design goals of the aforementioned studies were to create a freeform lens having a specific light pattern with higher lighting efficiency and uniformity of illumination. These freeform lenses could almost provide the lighting requirements for fishing. In this paper, to satisfy the lighting demands of both fishing and on-board activities on fishing boats, we propose a single, freeform secondary lens with a white LED to meet both requirements at the same time. In the design process, Gaussian decomposition is utilized to model the light distribution pattern of the proposed LFWL. Besides work in optics design and computer simulations, optical experiments are presented to show the advantages of the proposed LFWL.

II. DESIGN OF THE LFWL LENS

2.1. Gaussian Decomposition Method

The designed LFWL is employed for both fishing and on-board work. Correspondingly, the LIDC of the LFWL lens is designed to dedicate one central region for fishing, with two side lobes to cover on-board work, as presented in Fig. 1. The central region correlates with -20 to 20 degrees. Meanwhile, two side lobes correspond to -80 to -40 degrees and 40 to 80 degrees, having the same intensity level. The light within the side lobes is responsible for lighting the boat's front and rear surfaces for on-board work. To attract shoals of fish, the higher energy level should be focused on the central region instead of the side lobes.

The LIDC of the LFWL lens can be determined by using Gaussian decomposition [12, 13] as follows:

$$I_{Lens}(\theta)=\frac{a_0}{\sigma_0\sqrt{2\pi}}e^{-\frac{\theta^2}{2\sigma_0^2}}+\sum_{n=1}^{\infty}\frac{a_n}{\sigma_n\sqrt{2\pi}}\left(e^{-\frac{(\theta-\mu_n)^2}{2\sigma_n^2}}+e^{-\frac{(\theta+\mu_n)^2}{2\sigma_n^2}}\right) \quad (1)$$

where μ_0 indicates the position of the main lobe, while μ_n (n = 1, 2…) indicates the position of the n^{th} side lobe. The multiplication factors a_0, a_1, a_2,… and standard deviations σ_0, σ_1, σ_2,… are chosen to fit the desired LIDC pattern. The values of these parameters corresponding to the desired LIDC pattern are listed in Table 1. Moreover, the workflow for finding the desired parameters by Gaussian decomposition is displayed in Fig. 2, and its details are presented as follows.

***Step* 1:** Select the key parameters of the Gaussian mixtures based on the desired LIDC pattern: the number of side lobes, and the positions of the main lobe and all side lobes.

***Step* 2:** Estimate the widths of main and side lobes, then determine the parameters σ_n, for n = 1, 2, 3,…

***Step* 3:** Run the minimum mean-square error (MMSE) estimation algorithm to find the multiplication factors a_n.

***Step* 4:** If the MMSE is within the accepted tolerance, *i.e.* MMSE < ε, where $\varepsilon = 10^{-3}$ is the maximum acceptable error, then stop the procedure. Otherwise, go back to Step 2, adjust the values of σ_n, and repeat the algorithm.

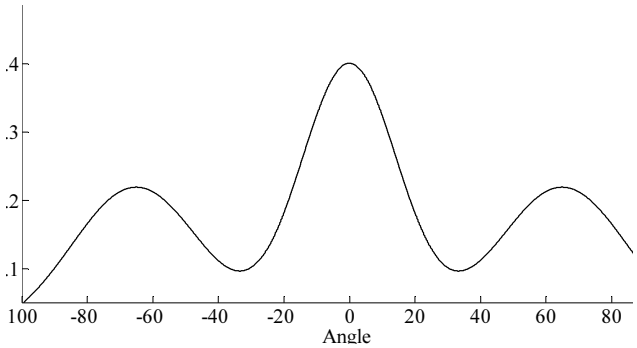

FIG. 1. The designed LIDC of the LFWL lens.

TABLE 1. Design parameters of the LIDC for a LFWL lens using Gaussian decomposition

Design Parameter	Values
a_0	15.04
a_1	10.98
μ_1	65
σ_0	20.35
σ_1	39.63

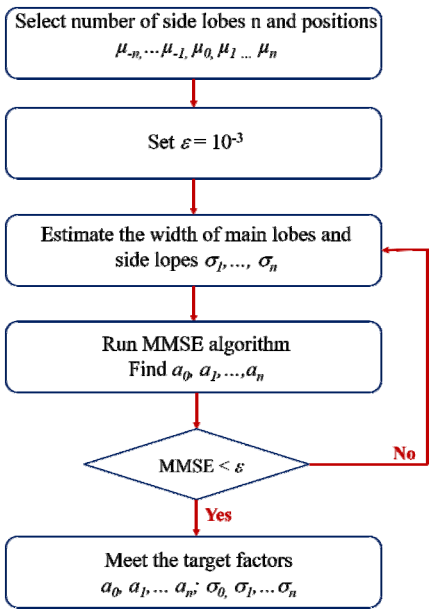

FIG. 2. Flowchart for finding the target factor using Gaussian decomposition.

Through the design workflow, the desired LIDC of a LFWL lens can be formed by the superposition of Gaussian functions with the proper parameters. Computing these parameters (listed in Table 1) results in the analytical solution of the LIDC proposed in Fig. 1.

2.2. Construction of the LFWL Lens

In this study, the Cree® XLamp® XP-E LEDs with viewing angle of 115 degrees are employed as the light engines to supply white light with a color temperature of 6500 K. Design of a freeform secondary lens is always related to the LED light source. The light-emission patterns of most LEDs can be considered to be correlated to the cosine function, so the normalized luminous intensity distribution curve (LIDC) of the light source can be calculated as follows:

$$I_{LED}(\theta) = I_a \cos^x(\theta) \tag{2}$$

where $I_{LED}(\theta)$ is the luminous intensity for each angle θ, I_a is the axial luminous intensity, and the exponential factor $x = -ln(2)/ln(\cos\Phi_{0.5})$.

By the law of energy conservation, the mapping relationships between the light-emission angles of LED and lens on a vertical surface, $I_{LED}(\phi)$ and $I_{Lens}(\phi)$, and between the light-emission angle of LED and lens on a horizontal plane, $I_{LED}(\theta)$ and $I_{Lens}(\theta)$, are determined. The total energy of the LED light passing through the LFWL lens is constant. Next, Snell's Law is used to obtain the normal vector corresponding to each point on the lens, and thus to construct the entire LFWL lens. The vector equation of Snell's Law [14] can be written as follows:

$$[n_0^2 + n_1^2 - 2n_0n_1(O \cdot I)]^{1/2} \cdot N = O \cdot n_0 - I \cdot n_1 \tag{3}$$

Here n_0, n_1 are refractive indices; O is the refraction unit vector; I is the incident unit vector; and N is the normal vector corresponding to the incident and refraction vectors.

The method or constructing the main curve of the LFWL lens is displayed in Fig. 3. The center of the LED source is located at the origin of a Cartesian coordinate system. The incident ray I_i ($i = 1, 2$) from the LED source is aimed at the main curve at the corresponding point R_i, to generate the refracted ray O_i. The points Q_i and R_i separate the main curve of the LFWL lens into four parts of the same arc length. The curves Q_0 Q_1 and Q_1 Q_2 are formed by the functions $f_1(x)$ and $f_2(x)$ respectively. The normal vector N_i can be obtained based on the derivative of $f_i(x)$. The end points of the main curve are preset as Q_i, which are the boundary conditions for Eq. (3), combined with the results for the $f_i(x)$ derivatives. Indeed, the curves Q_0 Q_1 and Q_1 Q_2 curves can be obtained by employing angular energy mapping between the LIDC of the lens (Eq. (1)) and the LIDC of the LED source (Eq. (2)), then substituting the mapping relationship into Snell's Law (Eq. (3)). First, the Zemax optics design program is employed to find $f_i(x)$. Moreover, by changing $f_i(x)$, N_i can be adjusted freely until O_1 and O_2 are directed to the desired LIDC of the LFWL lens. The original three-dimensional (3D) LFWL lens design is presented in Fig. 4.

III. RESULTS AND DISCUSSION

To conduct the proposed secondary lens design, the Solidworks program and optical design program Zemax are utilized. The optimal freeform surface generated by the above software is shown in Fig. 4.

The abovementioned white LED package, having a luminous flux of 107 lumens, serves as a light source in our simulations and experiments. This white-LED package is mounted on the optimized freeform lens to form the LFWL module for experiments. Using Solidworks, the LED

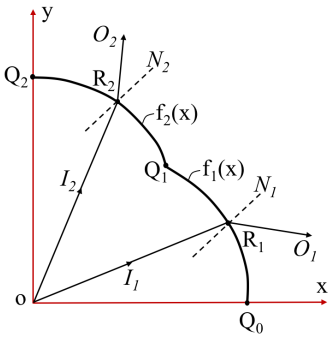

FIG. 3. Two-dimensional (2D) ray-tracing plot of the LFWL lens.

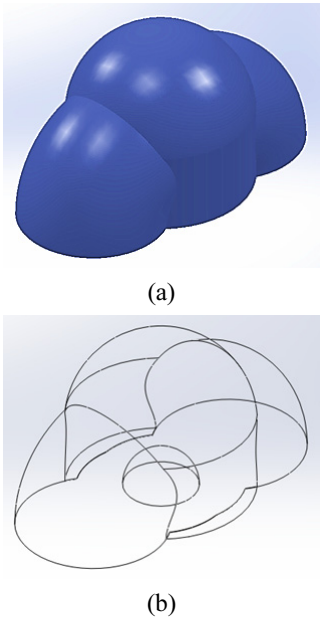

FIG. 4. (a) The 3D diagram of the obtained freeform lens for a fishing/working lamp, and (b) its 3D design geometry.

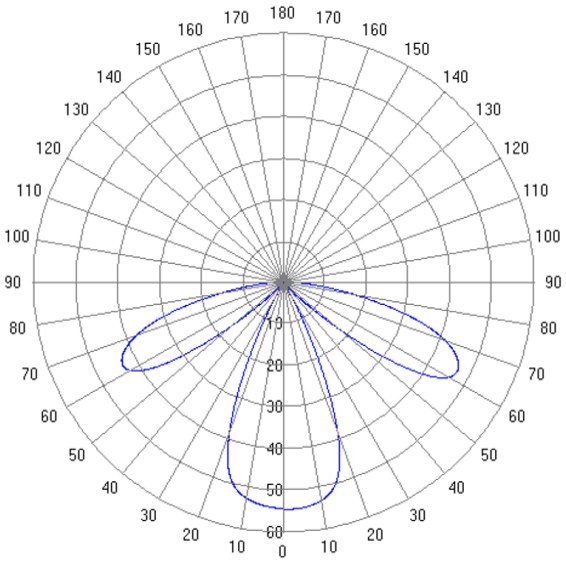

FIG. 5. The simulated 2D intensity distribution of the proposed LFWL lens.

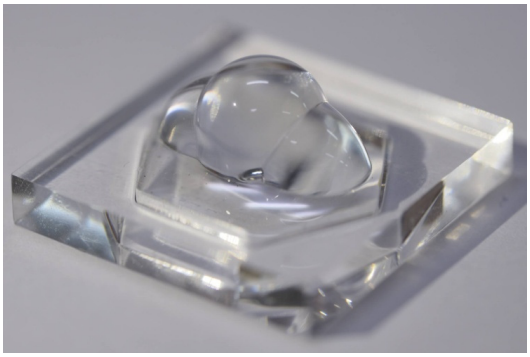

(a)

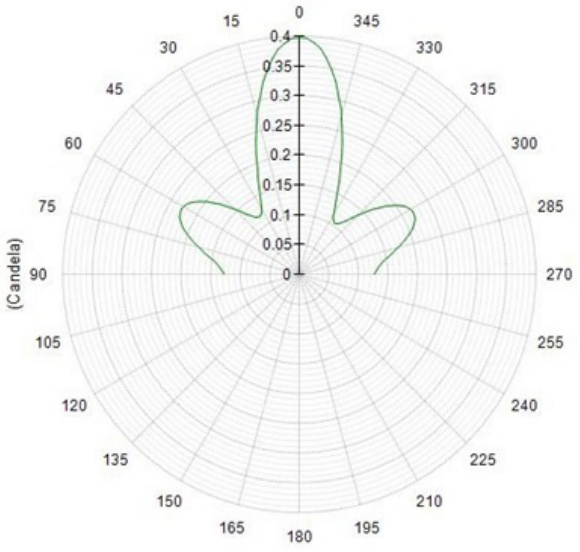

(b)

FIG. 6. (a) The fabricated freeform lens sample, and (b) its 2D intensity distribution map.

module is drawn as a mechanical model, which serves as input to the TracePro program for Monte Carlo ray-tracing, to evaluate the lighting performance. The simulated 2D intensity distribution of the proposed LFWL lens is displayed in Fig. 5. Here the light within 0-45 degrees is used for attracting fish, while that within 55-85 degrees (looking like a pair of bird wings) is for on- board lighting. The proposed LED fishing/working secondary lens is prototyped for optical experiments, as shown in Fig. 6(a). This prototype is made of acrylic according to the lens structure shown in Fig. 4. The 2D optical intensity distribution of the LFWL module is measured by a goniophotometer and shown in Fig. 6(b). Comparing the designed (Fig. 1) and measured (Fig. 7) LIDCs of the LFWL, we can conclude that these results are similar to each other. Therefore, the novel LFWL lens design using Gaussian decomposition is feasible.

Next, to compare the performance of our proposed free-

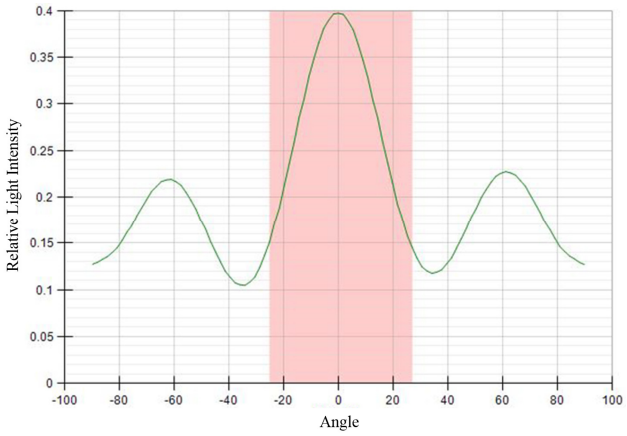

FIG. 7. The measured LIDC of the LFWL lens.

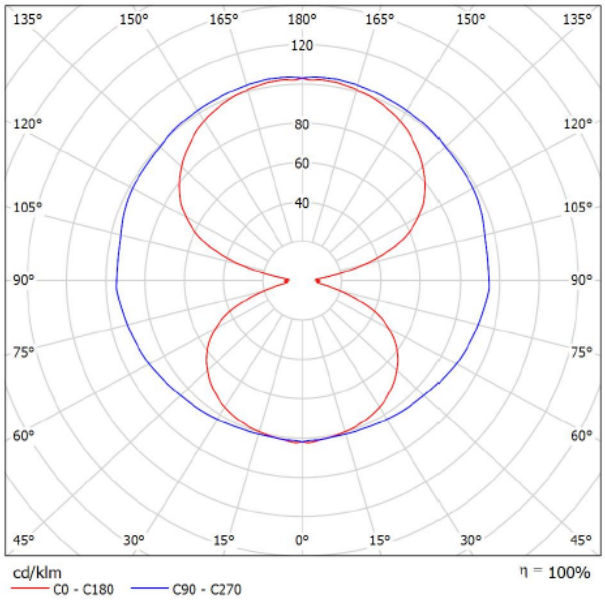

FIG. 8. The measured LIDC of the HID fishing lamp.

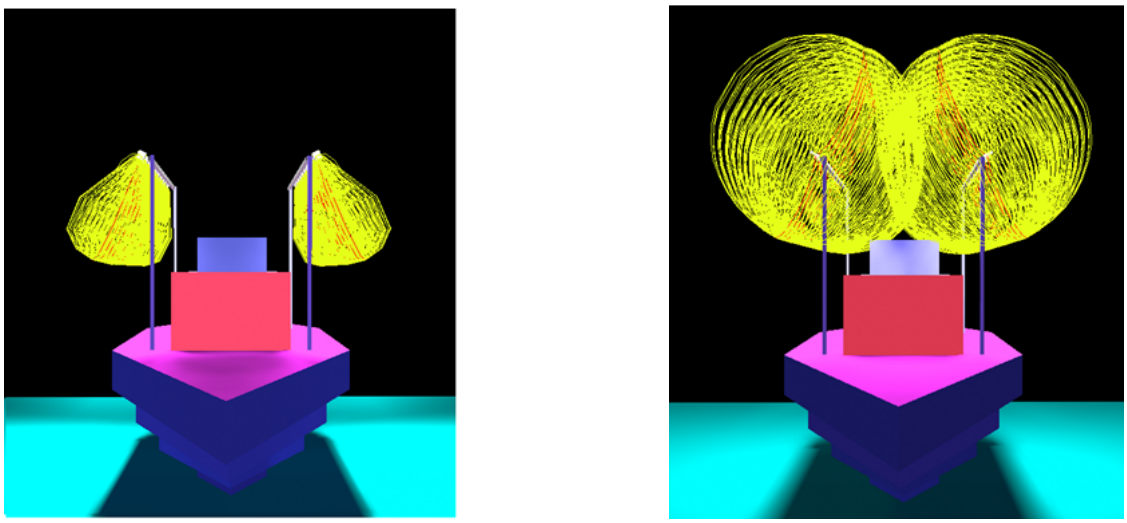

(a) (b)

FIG. 9. (a) Simulation of a fishing boat equipped with 30 sets of 450-W LED fishing/working lights; (b) simulation of a fishing boat equipped with 20 sets of 2000-W HID fishing lamps.

TABLE 2. Comparison of the lighting performances of the novel LED fishing lamps and the traditional HID fishing lamps for a fishing boat

Lamp systems	Power (W)	Deck (lux)	Sea surface (lux)	Underwater (lux)	Efficiency (%)
LED lamps	13,500	3065	1639	1315	91
HID lamps	40,000	2992	1768	1438	84

form lens to that of a conventional fishing light, a 22,5000 lumens/2000 W Philips HID conventional fishing lamp and a 54,000 lumens/450 W LED light composed of an array of the proposed fishing/working LED modules are investigated. Figure 8 illustrates the measured light distribution curve of the HID fishing lamp.

Regarding the configuration of fishing and working environments, in our simulations we consider two 12 m (L) × 3 m (W) fishing boats with a board of 2 m higher than the water surface. One boat is equipped with 30 sets of the proposed 450-W LED fishing/working lights, as shown in Fig. 9(a); the other is equipped with 20 sets of the 2000-W HID fishing lamps, as shown in Fig. 9(b). The lamps are hung on poles that are located on both sides of the fishing boat, equally spaced to each other and 2 m above the deck.

To evaluate the illumination distribution, we use Dialux lighting design software to process the intensity distribution file (IES file) for each type of light, which is obtained by optical measurements using a goniometer. The mean illuminance values on the deck and on the water's surface around the fishing boat are presented in Table 2. It can be observed that the proposed lamp consumes only 1/3 as much electrical power as the traditional HID lamp, but yields almost the same illumination distribution, on boat or water.

To study further the lighting performance for attracting fish in the water, we investigate the underwater lighting effect with the Zemax program. The mean illuminance results are presented in Table 2. The computation takes account of seawater absorption, seawater surface reflectivity, and the light spectrum, to yield illumination distribution data at a depth of 1 meter underwater. According to the simulation data, we can find that the seawater transmission efficiency of the novel fishing/working lamps is 91%, while that of the traditional HID fishing lamp is 84%.

This result confirms that the proposed LED light performs more efficiently, and should attract fish shoals more capably than the traditional light under the water's surface. The simulated data for these lamps are all given in Table 2.

IV. CONCLUSIONS

In this paper, a novel method for freeform lens design for LED fishing/working lamps is proposed. Gaussian decomposition is employed to represent the LIDC of the LFWL lens. This method plays an important role in the LFWL lens design. Using Snell's Law and energy conservation, with the Solidworks, Zemax, and TracePro programs, the surface of the LFWL lens can be determined and optimized. Our experimental results demonstrate that the fishing/working lamp can replace a traditional HID fishing lamp, to serve both fishing and on-board working purposes with lower power consumption. According to the simulation

results, the proposed fishing/working lamps can achieve better illumination performance as well as threefold power savings, compared to traditional HID lamps.

ACKNOWLEDGMENT

This research is funded by Vietnam National Foundation for Science and Technology Development (NAFOSTED) under grant number 103.03-2015.62.

REFERENCES

1. J. S. Yang, J.-H. Park, B.-H. O, S.-G. Park, and S. G. Lee, "Design method for a total internal reflection LED lens with double freeform surfaces for narrow and uniform illumination," J. Opt. Soc. Korea **20**, 614-622 (2016).
2. B.-Y. Joo and J.-H. Ko, "Analysis of color uniformity of white LED lens packages for direct-lit LCD backlight applications," J. Opt. Soc. Korea **17**, 506-512 (2013).
3. W.-S. Sun, C.-L. Tien, J.-W. Pan, T.-H. Yang, C.-H. Tsuei, and Y.-H. Huang, "Simulation and comparison of the lighting efficiency for household illumination with LEDs and fluorescent lamps," J. Opt. Soc. Korea **17**, 376-383 (2013).
4. M.-F. Lai, Y.-C. Chen, N. D. Q. Anh, T.-Y. Chen, H.-Y. Ma, and H.-Y. Lee, "Design of asymmetric freeform lens for low glared LED street light with total internal reflection," Opt. Express. **24**, 1409-1415 (2016).
5. R. Hu, X. B. Luo, H. Zheng, Z. Qin, Z. Q. Gan, B. L. Wu, and S. Liu, "Design of a novel freeform lens for LED uniform illumination and conformal phosphor coating," Opt. Express. **20**, 13727-13737 (2012).
6. J.-J. Chen, Z.-Y. Huang, T.-S. Liu, M.-D. Tsai, and K.-L. Huang, "Freeform lens design for light-emitting diode uniform illumination by using a method of source-target luminous intensity mapping," Appl. Opt. **54**, E146-E152 (2015).
7. K. C. Lin, "Illumination variation under a freeform lens and misalignment of light source," in *Proc. 6th IEEE Conference on Industrial Electronics and Applications* (Beijing, China, June 2011), pp. 1079-1084.
8. D. Ma, Z. Feng and R. Liang, "Deconvolution method in designing freeform lens array for structured light illumination," Appl. Opt. **54**, 1114-1117 (2015).
9. B. Xie, R. Hu, Q. Chen, X. J. Yu, D. Wu, K. Wang, and X. B. Luo "Design of a brightness-enhancement-film-adaptive freeform lens to enhance overall performance in direct-lit light-emitting diode backlighting," Appl. Opt. **54**, 5542-5548 (2015).
10. S. C. Shen and H. J. Huang, "Design of LED fish lighting attractors using horizontal/vertical LIDC mapping method," Opt. Express. **20**, 26135-26146 (2012).
11. S. C. Shen, J. S. Li, and H. C. Huang, "Design a light pattern of multiple concentric circles for LED fishing lamps using Fourier series and an energy mapping method," Opt. Express. **22**, 13460-71 (2014).
12. W. Wagner, A. Ullrich, V. Ducic, T. Melzer, and N. Studnicka, "Gaussian decomposition and calibration of a novel small-footprint full-waveform digitising airborne laser scanner," ISPRS J. Photo. Remote Sensing **60**, 100-112 (2006).
13. R. R. Lindner, C. V. Ciro, C. E. Murray, S. Stanimirović, B. Babler, C. Heiles, P. Hennebelle, W. M. Goss, and J. Dickey, "Autonomous gaussian decomposition," The Astronomical Journal **149**, 1-12 (2015).
14. J. H. Wang, Y. C. Liang, and M. Xu, "Design of a see-through head-mounted display with a freeform surface," J. Opt. Soc. Korea **19**, 614-618 (2015).